Damage tolerant cork based composites for aerospace applications

J. M. Silva **C. Z. Nunes** **N. Franco** **P. V. Gamboa**
jmas@ubi.pt
Department of Aerospace Sciences
University of Beira Interior
Covilhã, Portugal

ABSTRACT

This work aims at improving the resilience and damage tolerant properties of CFRP by using cork, which is a natural material with good energy absorption capacity and thermal insulating and vibration damping characteristics. Two types of materials were considered: a sandwich formed by carbon-epoxy facesheets with a cork-epoxy core and a carbon-epoxy laminate with embedded cork granulates. The damage tolerant properties were evaluated by low velocity impact tests according to the type of material. Additionally, this work intends to evaluate the feasibility of using a cork agglomerate combined with CFRP in a sandwich configuration in order to improve the aeroelastic properties of certain types of aerospace components aiming at preventing the occurrence of damage due to flutter. A computational analysis was used to determine the critical flutter speed of a cork based sandwich plate and other conventional materials, such as aluminium alloy and CFRP.

Results are clear about the benefits of using cork based composites either by improving the damage tolerant properties under impact loading or by extending the flight envelope without weight penalty by increasing the flutter critical speed.

NOMENCLATURE

AIC	Aerodynamic Influence Coefficient matrix
C	damping matrix
CFRP	Carbon Fibre Reinforced Plastic
D	generalised vector of nodal degrees of freedom
E_a	absorbed energy at time t (J)
E_f	elastic modulus (GPa)
E_i	impact energy (J)
f	frequency (Hz)
F	impact contact force at time t (N)
F_a	aerodynamic forces produced by structural deformation (N)
FE	finite element
FRP	Fibre Reinforced Plastic
g	acceleration due to gravity ($9{\cdot}81 ms^{-1}$), damping
h	structural deformation
K	stiffness matrix
L_h	aerodynamic force vector
m	impactor mass, plate mass (kg)
M	mass matrix
PMI	polymethacrylimide
q	generalised co-ordinates
q_∞	freestream dynamic pressure (Pa)
R_{ext}	external loads
t	time (s), thickness (m)
v	impactor velocity at time t (ms^{-1})
V	speed (ms^{-1})
V_f	flutter speed (ms^{-1})
v_i	impact velocity (ms^{-1})

Symbols

δ	impactor displacement at time t (m)
δ_i	impactor displacement from reference location at $t = 0$ (m)
ν	Poisson's ratio
ω	natural frequency of vibration (Hz)
σ_r	static flexural strength (MPa)
Δ	variation in parameter

Paper No. 3695. Manuscript received 17 November 2010, revised version received 25 March 2011, accepted 14 April 2011.

https://doi.org/10.1017/S0001924000006205 Published online by Cambridge University Press

1.0 INTRODUCTION

The design of aerospace structures and components is driven by strict weight saving and improved specific strength requirements. Additionally, the emerging environmental global concerns lead to the continuous development of lighter and more efficient aircraft, which depend largely on the availability of new types of materials and related technologies. The choice for a new material for airframe application must ensure that no compromises are made in terms of the reliability and durability of the components, contributing to the maximisation of the mandatory flight safety requirements.

Composite materials, particularly fibre reinforced polymer based materials (FRP), represented a giant step in the evolution of the aerospace industry since the 1960-70s[1], as they introduced new opportunities in the design of aircraft structures. However, even with remarkable mechanical properties, composite materials have some drawbacks that can limit its usage under certain types of operational conditions. One of these limitations is the low energy absorption capacity of FRP, namely those reinforced with carbon fibres (CFRP) which are widely used in aerospace applications. In fact, CFRP experience very little plastic deformation when facing low velocity impact loads that can be imposed by foreign objects or careless handling. In this case, the damage mechanisms for dissipating energy are mainly caused by matrix cracking, fibre breakage and delamination[2]. There are some options for improving the low velocity impact response of CFRP, which can result from the toughening of the fibre, matrix or interface and hybridisation, which consists in the utilisation of high strain energy fibres in addition to the original reinforcement fibres of the composite. Some researchers have driven their attention towards the enhancement of the energy absorption capacity of the matrix of the composite material through the addition of rubber or thermoplastic compounds[3-5].

The present work explores the possibility of using carbon-epoxy laminates combined with cork aiming at improving the resilience and damage tolerant properties of this type of composites. Cork is a natural material with excellent thermal insulation and energy absorption properties which explain its use for centuries in common applications, such as cork stoppers and insulation boards[6]. However, the intrinsic cellular morphology of this natural material suggests that cork based agglomerates can be an alternative choice to other types of core materials. In fact, cork cells are strong and the specific strength of cork is comparable to some rigid synthetic foams[7]. In addition, cork based materials are used for a long time in components under dynamic loading for the suppression of vibrations as a result of their excellent damping characteristics. As a consequence of these characteristics, one can think of the possible use of cork based composites in aerospace components that may be particularly affected by impact loads or vibrating conditions imposed by aeroelastic phenomena (such as flutter). In fact, there are currently some aerospace applications of cork based composites used for thermal shielding purposes for launchers fairings due to their high damage tolerance under impact loading[8].

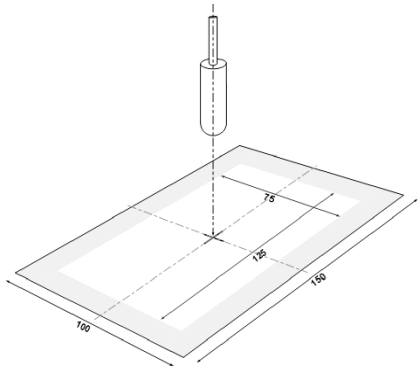


Figure 1. Schematic representation of the impact region of carbon-epoxy laminates with embedded cork granulates.

This paper presents experimental results for low velocity impact tests performed with two types of cork based composites: a sandwich formed by carbon-epoxy facesheets with a cork-epoxy core and a carbon-epoxy laminate with embedded cork granulates. The first option came as a natural result of the benefits of using a sandwich type configuration in aircraft components, since it provides improved mechanical behaviour and damage tolerant properties under certain loading conditions. In this case, the properties of primary interest for the core material are low density, high shear modulus, high shear strength, elevated stiffness perpendicular to the faces and good thermal and acoustic insulation characteristics[9,10]. These requirements can be met by using cork-epoxy agglomerates with enhanced mechanical properties for the core material, which were developed as an alternative to conventional cork agglomerates in the course of a previous work of the authors[11,12].

The embedded cork granulates within conventional carbon-epoxy laminates aims at giving better resilient properties to this typically brittle material. However, cork granulates may act as elastic inclusions in the host material and therefore lead to a decrease in its strength limit under static loading.

Finally, this work also intends to evaluate the feasibility of using a cork agglomerate combined with CFRP in a sandwich structure in order to increase the structural eigenvalues and, consequently, critical flutter speed and frequency. The main goal is to reduce the weight of the structure for a given flight envelope without changing dramatically the structural strength of the component. It is believed that the use of a cork based material may have a contribution in flutter suppression not only because it will increase the second moment of area of the structure but also due to this material's natural damping characteristics.

2.0 MATERIAL AND METHODOLOGY

2.1 Materials

As mentioned before, a new type of cork-epoxy composite with enhanced mechanical properties was developed in a previous work of the authors[12], allowing to obtain better overall mechanical properties under static loading when compared to conventional cork agglomerates. The challenge in the preparation process of these agglomerates was related with the effective agglomeration method and the right cork/resin ratio necessary to obtain an optimised specific strength for core material applications. In the case of the sandwich specimens used in this research, the facesheets were obtained through a hand layup process consisting of three plies of a 196g/m^2 carbon fibre fabric with orientation (0º/90º/0º) embedded with epoxy resin. The cork agglomerates used in the core were obtained from a mixture of cork granulates (size 2/4) with epoxy resin. This mixture is then put into a steel mould and submitted to a 50bar pressure (using a hydraulic press machine) at room temperature and for two hours. After this, the mould is placed in a heater at a constant temperature of 60ºC for 6 hours to ensure a convenient post-curing stage. Two core thicknesses were obtained from this process: 20mm and 30mm. In each case, the cork-resin proportion was adjusted to get the same density of the agglomerate (260kg/m^3).

The geometry of these sandwich type specimens take into account both the impact and post-impact test requirements. In fact, in the absence of a specific standard impact test method for sandwich structures, the dimensions of the impact specimens (190mm × 70mm) resulted as a constraint of the subsequent residual strength tests (under flexural mode), which in turn were performed according to the recommendations of ASTM C393/C393M[13]. Nevertheless, the general requirements of the impact tests followed the recommendations of ASTM D7136/D7136M[14] with minor adjustments.

https://doi.org/10.1017/S0001924000006205 Published online by Cambridge University Press

The other type of cork based composites used in this work were obtained from a conventional carbon-epoxy laminate fabricated in autoclave with embedded cork granulates. The geometry of the specimens used for impact tests followed the recommendations expressed in ASTM D7136/D[14], having a rectangular shape with 150mm × 100mm. According to this standard, the thickness of the specimen must be comprised between 4mm to 6mm. In this case, a 5mm thickness was obtained through manual stacking of 28 plies of Texipreg HS 160 REM prepreg. All the plies were oriented parallel to the longitudinal axis of the specimens, and cork granulates were embedded between the 4th-5th plies and 23rd-24th plies. Two cork granulate sizes were considered: small (0·5mm) and medium (0·9mm). Figure 1 shows the window available for the impact event considering the region of the specimen that is fixed to the support of the impact apparatus (grey border).

Prior to the impact tests of the cork based laminates, a set of static flexural tests were undertaken in order to assess the possible detrimental effect of the embedded cork granulates in the static mechanical behaviour of the host material. Three-point flexural tests were performed according to ASTM D790[15], resulting in a 150mm × 25mm rectangular specimen geometry. The thickness of the specimens is a consequence of the number of plies and the cork granulate size. Since a total of 10 plies were used in this case, the nominal thickness of the specimens varied between 1·56mm (without cork) and 1·7mm (considering two layers of small cork granulates placed between the 3rd-4th plies and the 7th-8th plies).

Table 1 presents the average results obtained from the flexural tests of five specimens for each type of material. It is clear that cork has a detrimental effect in the overall mechanical characteristics of the composite material under static loading. In fact, the flexural strength limit and the elastic modulus were decreased by 19·8% and 7·9%, respectively, when comparing the specimens with and without cork granulates.

Table 1
Variation of the static flexural strength of the cork-epoxy laminates with and without cork granulates

Specimen	σ_r, MPa	$\Delta\sigma_r$, %	E_f, GPa	ΔE_f, %
$[0^o_{10}]$	1,628·0	–	112·9	–
$[0^o_3/cork/0^o_2]s$	1,316·3	–19·8	106·0	–7·9

Finally, the passive solution for flutter suppression described in this work consists of a 500mm × 150mm sandwich plate with a 1mm thick cork core and one 0·2mm layer of woven carbon/epoxy at each facesheet.

2.2 Equipment details

A drop tower apparatus with a free-falling mass was used to impact the sandwich plates. The hemispherical impactor surface had a radius of 20mm and the dropped carriage had a total mass of 3kg. The energy of impact was adjusted through the choice of different departure heights of the falling mass. The specimens were constrained in each lateral side using a fixed support and the impact window was chosen according to the intended damage zone for each specimen's geometry. In fact, carbon-epoxy laminates were impacted in the middle-point as shown in Fig. 1, but the impact window of the sandwich components was moved to the middle-point of the semi-span distance due to the requirements of the subsequent residual strength flexural tests. In both cases, impact forces were acquired with a piezoelectric transducer located between the impactor and the carriage.

In the case of sandwich specimens, four-point flexural tests were made to quantify the residual strength after impact using a servo-hydraulic machine with a 100kN load capacity. During these tests, particular attention was paid towards the minimisation of local damage caused by the contact of the hemi-spherical actuators of the machine and the material; small rubber pads were used for this purpose.

2.3 Computational analysis

As mentioned before, another goal of the present work is to study the feasibility of using cork based composites for flutter suppression. A preliminary approach on this subject was made through a computational analysis of the aeroelastic properties of a 500mm × 150mm sandwich plate with a cork core and carbon-epoxy facesheets. A computational model was built using the finite element (FE) code ANSYS®. This software was used in combination with another code, ZAERO®, to study the dynamic and aeroelastic behaviour of this structure. These results were then compared to 6061-T6 aluminium alloy and carbon-epoxy plates 0·75mm and 1·4mm thick, respectively. These thicknesses were chosen such that the flight envelope of the three structures would be approximately the same in order to focus the analysis on the weight of the components.

3.0 EXPERIMENTAL RESULTS

3.1 Sandwich structures

Four levels of energy were considered for characterising the low velocity impact behaviour of sandwich specimens: 5J, 10J, 15J and 20J. The dynamic response of the material was assessed using *Force vs Time* and *Energy vs Time* graphs. The impact force comes as a direct measurement from the load cell connected to the impactor. The drop tower apparatus is digitally controlled and has specific data acquisition software which converts the impact force into the absorbed energy following the expressions recommended in ASTM D7136/D7136M-05[14]:

$$E_i = \frac{mv_i^2}{2} \quad \ldots (1)$$

$$\delta(t) = \delta_i + v_i + \frac{gt^2}{2} - \int_0^t \left(\int_0^t \frac{F(t)}{m} \mathrm{d}t \right) \mathrm{d}t \quad \ldots (2)$$

$$E_a(t) = \frac{m\left(v_i^2 - v(t)^2\right)}{2} + mg\delta(t) \quad \ldots (3)$$

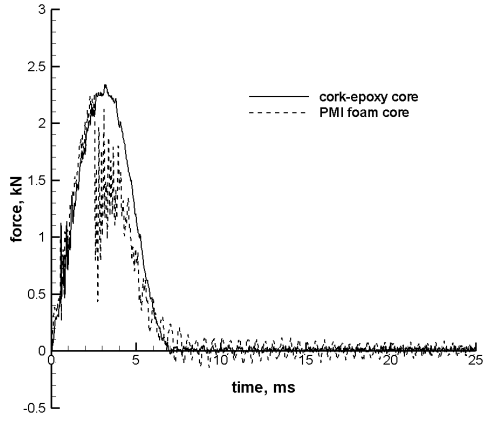
where E_i is the impact energy, m is the impactor mass, v_i is the impact velocity, g is the acceleration due to gravity (9·81ms^{-1}), v is the impactor velocity at time t, F is the impact contact force at time t, δ_i is the impactor displacement from reference location at $t = 0$, δ is the impactor displacement at time t and E_a is the absorbed energy at time t.

For comparative purposes, the impact tests were reproduced with another core material, a polymethacrylimide (PMI) foam, which has benchmark properties for applications in aerospace sandwich components.

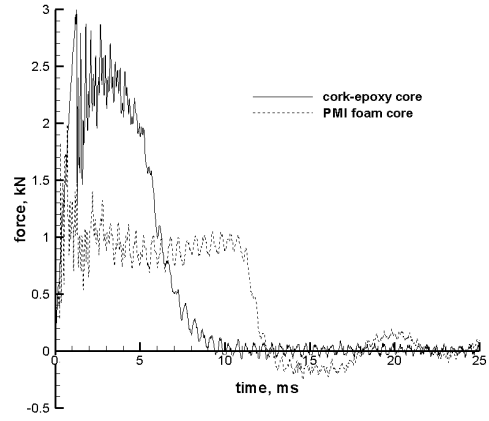
Figure 2 shows the impact tests results in the form of *Force vs Time* graphs for the two types of materials and considering the extreme values of the energy of impact: 5J and 20J. These results refer to the highest value of the thickness of the core (30mm) since they are very similar to the ones of the lowest thickness (20mm). From these graphs, some immediate conclusions can be highlighted: 1) cork based materials have a smoother response when compared to PMI foam, which is shown by the lower amplitude oscillations during the impact event; 2) in the case of PMI foam, there is a pronounced decrease of amplitude after the force peak has been reached.

The first conclusion corroborates the initial supposition about the excellent intrinsic damping properties of cork, which is still more evident for the highest level of energy of impact. On the other hand, the sudden variation of the impact force in the PMI specimens is a

https://doi.org/10.1017/S0001924000006205 Published online by Cambridge University Press



(a) 5J



(b) 20J

Figure 2. Force-time curves obtained for sandwich specimens with cork-epoxy or PMI cores considering two levels of energy of impact; (a) 5J; (b) 20J.

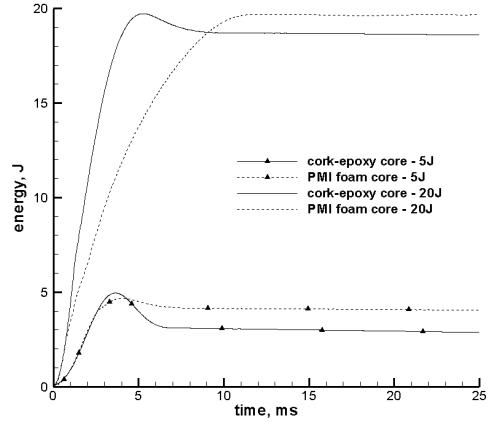


Figure 3. Energy-time curves obtained for sandwich specimens with cork-epoxy or PMI cores considering two levels of energy of impact (5J and 20J).

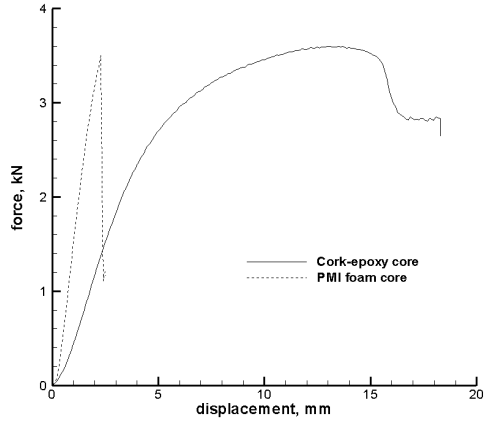


Figure 4. Comparison of the force-displacement curves obtained from flexural testing of cork-epoxy and PMI sandwich specimens.

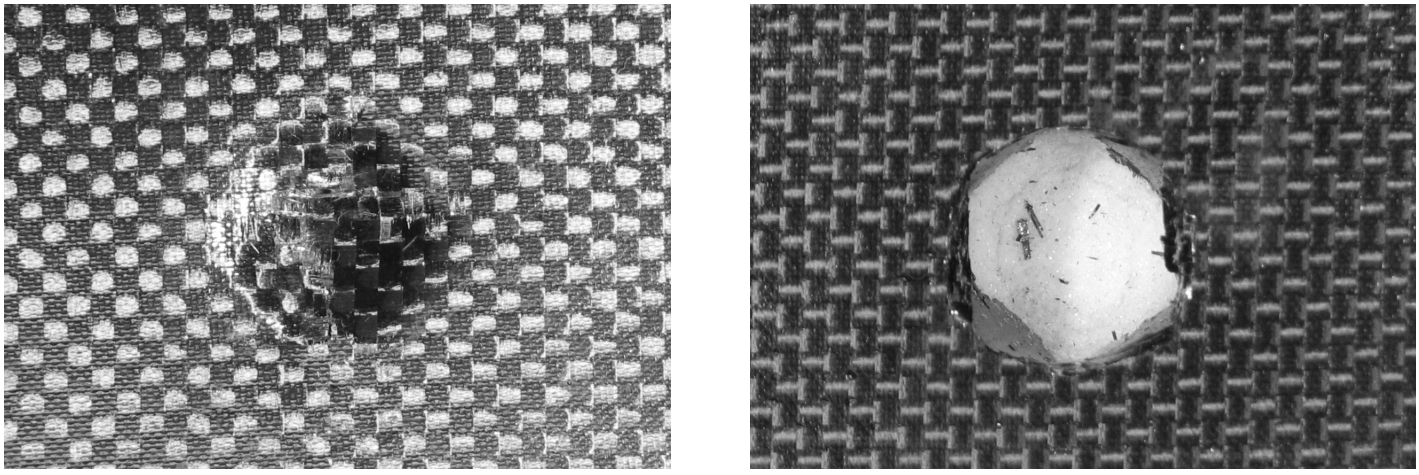
direct consequence of the occurrence of a damage mechanism, which can be either related with the facesheet or core materials.

During the impact event, a part of the total energy is absorbed by the material and transformed into some form of permanent damage or inducing an irreversible plastic deformation. Another part of this energy causes elastic deformation and vibration occurrence. Therefore, the total energy of impact can be divided into two categories: absorbed or dissipated energy. The damage tolerance of a certain material can thus be related with its energy absorption capacity without damage occurrence. This capacity becomes clear through the use of the *Energy × Time* curve represented in Fig. 3. As we can see, the PMI foam core material absorbs almost all the energy of impact (resulting into a plateau after the energy peak), whilst the cork based core shows a significant energy release after the energy peak has been reached. This effect is more pronounced for the highest value of energy of impact (20J), and in this case it was found that the impactor did not rebound after reaching the surface of the material, which is a clear indicator of the total energy absorption by the PMI foam in the form of damage.

The damage tolerant properties of the cork based core is also a consequence of its ductile behaviour under deformation, resulting into an obvious yielding region and large strains preceding the final rupture of the material. This behaviour is expressed by the *Force vs Deformation* curve in Fig. 4, which was obtained from a flexural test of a carbon-epoxy sandwich with a cork-epoxy agglomerate core. On the other hand, the PMI foam core has a more brittle characteristic, showing almost no signs of plastic deformation till its final rupture.

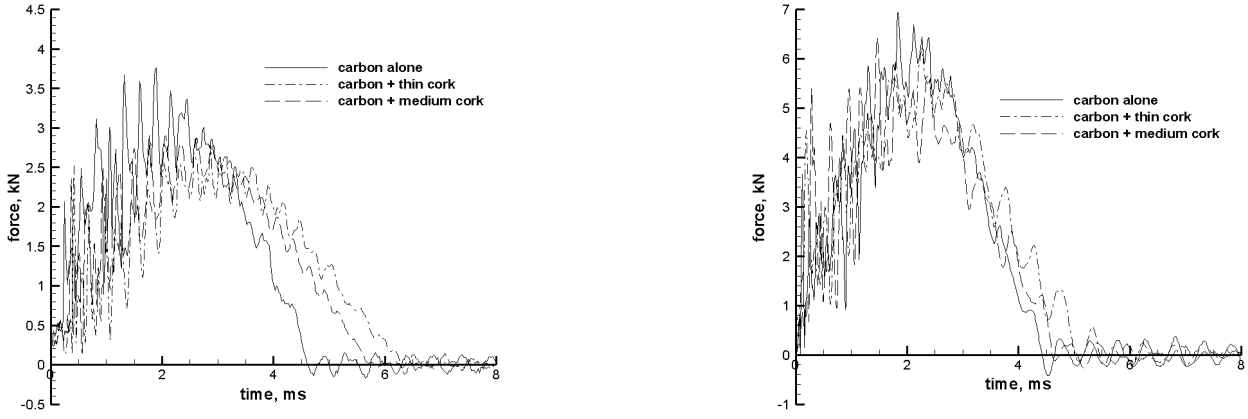
Post-impact residual strength tests allowed to confirm the superior damage tolerant properties of cork based sandwich components. Table 2 presents the ultimate loads of the two materials obtained from four-point bending tests considering both impacted (5J and 20J) and non-impacted specimens. In the case of the cork based cores, two different thicknesses were considered: 20mm and 30mm. The first immediate conclusion of these tests is the marked strength reduction after impact in the PMI sandwiches for all the energy levels, reaching about 19% in the case of the 20J impact event. The maximum reduction of the ultimate load verified for the cork-epoxy cores for the same energy level was about 12% in the case of the lower thickness specimens (20mm). However, an unexpected residual strength increase was found in the case of the 30mm thickness cork-epoxy specimens, reaching around 14% for the highest energy level. This apparently odd fact confirms the damage tolerance capability of cork based composites, since it seems that this type of material is not sensitive to the damages caused by the impact event for the energy range considered in these tests. Moreover, this energy absorption capacity of cork-epoxy cores has also a protective effect regarding the extension of damage of the facesheets. In fact, Fig. 5 shows that there was no full perforation of the carbon-epoxy facesheets in cork based sandwiches (Fig. 5(a)), whereas PMI foam core result into a complete penetration of the impactor and a consequent deeper extension of damage (Fig. 5(b)).

https://doi.org/10.1017/S0001924000006205 Published online by Cambridge University Press



(a) (b)

Figure 5. Image of the damage extension at the surface of the material after a 20J impact event: (a) cork-epoxy core; (b) PMI foam core.



(a) 5J (b) 15J

Figure 6. Force-time curves obtained from impact testing of carbon-epoxy laminates, with and without cork granulates, considering two energy levels; (a) 5J; (b) 15J.

Table 2
Load limit obtained for the different materials from the post-impact residual strength bending tests (*t* ≡ thickness of the specimen)

Material	without, kN	5J impact, kN	20J impact, kN
Cork-epoxy *t* = 20mm	2·24	2·42	1·97
Cork-epoxy *t* = 30mm	3·24	3·53	3·70
PMI foam *t* = 30mm	4·58	3·22	3·72

3.2 Carbon fibre laminates with cork

As mentioned before, the carbon-epoxy laminates with embedded cork granulates were tested with three levels of energy of impact: 5J, 10J and 15J. Again, *Force vs Time* and *Energy vs Time* plots were used to evaluate the behaviour of this type of material.

Figure 6 shows the *Force vs Time* response for the lowest and highest energy levels and considering two types of granulate size (small and medium). An apparent damping effect can be attributed to the presence of the cork granulates since the related plots show a lower amplitude of oscillations. This effect is more evident in the case of the medium size granulate and it seems to become less noticeable as the energy level increases.

Another interesting observation is the occurrence of a first peak force decrease which can be detected through the magnification of the *Force vs Time* plot. This peak is often related to the onset of a delamination damage which is a common failure mechanism of composite materials and it has been identified by other authors in similar materials[8]. From the analysis of the curves for all the energy levels, the introduction of the cork granulates causes a slight delay in the occurrence of this peak and, therefore, in the initiation of the delamination process.

Figure 7 presents the Energy *vs* Time curve considering the highest energy of impact (15J). As we can see, cork based laminates evince a higher level of absorbed energy, which seems to be unaffected by the granulate size. In fact, it was expected that the inclusion of a cork layer in the interior of the laminate could act as a barrier to the propagation of the energy waves resulting from the impact event. The results expressed by this energy curve demonstrate an effective energy absorption capacity. However, this conclusion requires a complementary evaluation to make certain that this energy increase implies a reduction in the level of damage within the material. In order to do so, the damage extension of the

https://doi.org/10.1017/S0001924000006205 Published online by Cambridge University Press

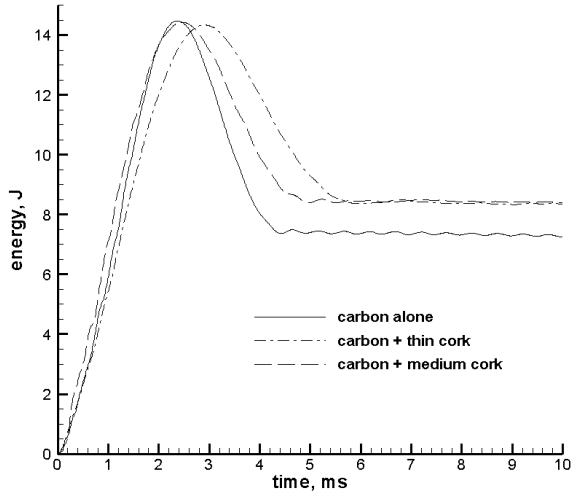
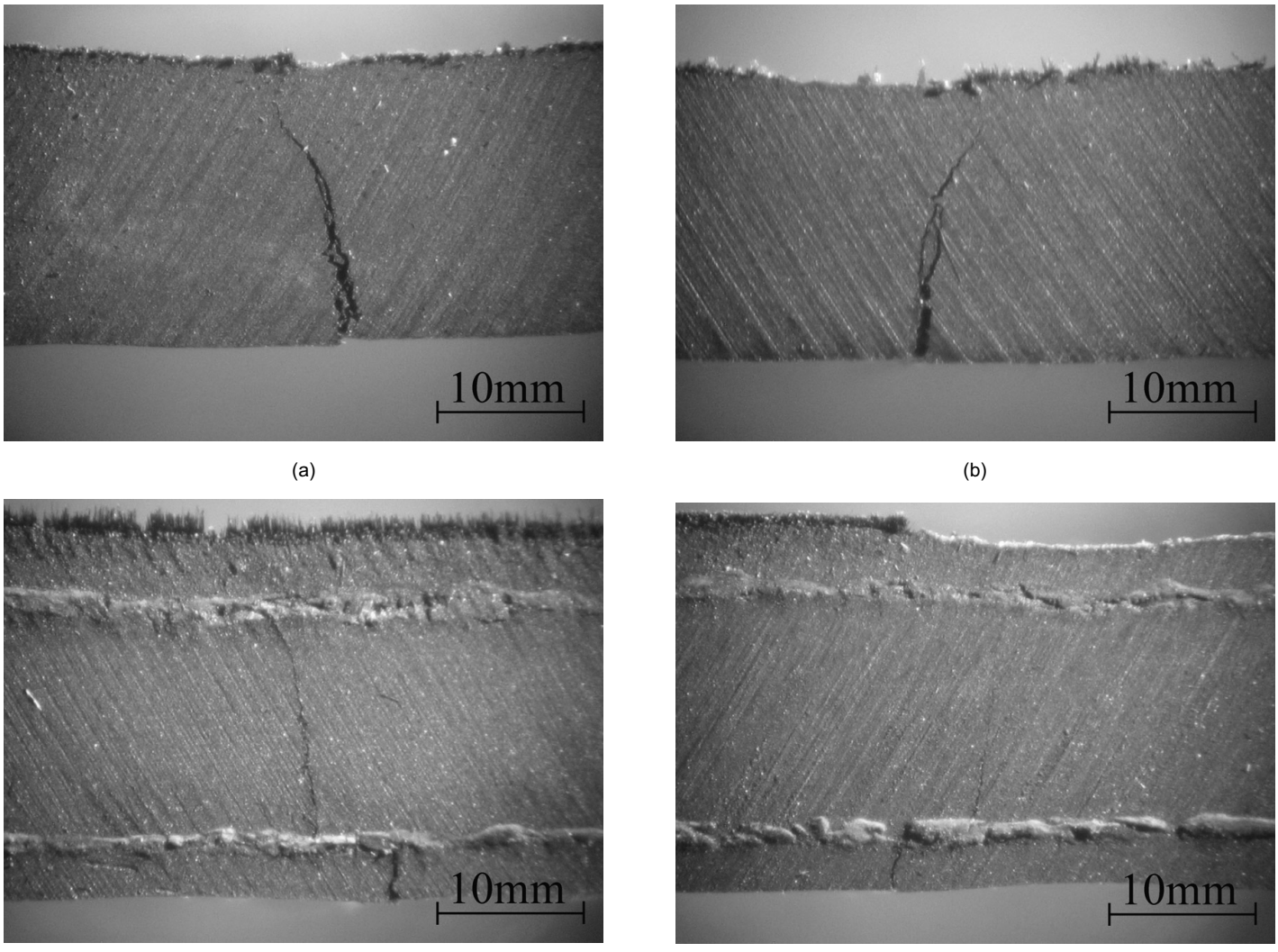


Figure 7. Energy-time curve obtained from impact testing of carbon-epoxy laminates, with and without cork granulates, for a 15J energy level.

impacted laminates with and without cork was assessed from microscopy observation of the section of the specimens in the vicinity of the impact region. The images shown in Fig. 8 were obtained from the observation of the cross-section of the two types of specimens (with and without cork granulates) after being impacted with an identical energy level (15J). The extension of damage was evaluated at two sections located at different distances from the point of contact of the impactor (10mm and 20mm). These images are clear about the advantageous contribution of the cork granulates for the minimisation of the damage extension, both in the thickness and in the laminate plane directions. In fact, the image of the farthest cross-section to the impact region shows that cork based laminates have a barely visible damage in contrast to the obvious crack extension of plain carbon-epoxy laminates. This effect is more perceptible in the case of those laminates having medium size cork granulates.

Another interesting conclusion is the change of path of the crack front caused by impact due to the presence of the thin cork layer, which seems to indicate that this material acts like a stop arrester against the sudden propagation of impact waves. This corroborating fact allows concluding that cork promotes the increase of the energy absorption limits of the usually brittle carbon-epoxy laminates and, therefore, reduces the damage level under low velocity impact loading.



(a) (b)

(c) (d)

Figure 8. Images of the cross-sections of the specimens showing the internal damage extension at two distinct positions from the impact point; (a) carbon-epoxy, 10mm; (b) carbon-epoxy, 20mm; (c) laminate with cork, 10mm; (d) laminate with cork, 20mm. Magnification 64x.

https://doi.org/10.1017/S0001924000006205 Published online by Cambridge University Press

4.0 FLUTTER ANALYSIS

4.1 Aeroelastic modelling

The flutter study uses complex eigenvalue analysis to determine the combination of airspeed and frequency for which the neutrally damped oscillatory motion is sustained. The computational analysis of this phenomenon requires the following steps: building the structural model and performing a modal analysis; generating aerodynamic grid points; computing aerodynamic matrices; providing connection between the structural and aerodynamic models; and, finally, solving the flutter equations. These steps are briefly explained in the following paragraphs.

4.1.1 Structural model

The basic principle for this type of dynamic analysis is the Newton's second law for a structure with multiple degrees of freedom:

$$[\mathbf{M}]\{\ddot{\mathbf{D}}\}+[\mathbf{C}]\{\dot{\mathbf{D}}\}+[\mathbf{K}]\{\mathbf{D}\}=\{\mathbf{R}_{\text{ext}}\} \quad \ldots (4)$$

where [**M**], [**C**] and [**K**] are the mass, damping and stiffness matrices, respectively, {**D**} is a generalised vector of the nodal degrees of freedom, and {$\mathbf{R}_{\text{ext}}$} is a vector of external loads applied to the structure. Since for undamped free vibration the damping is assumed to be zero and there are no externally applied loads, Equation (4) can be reduced to;

$$[\mathbf{M}]\{\ddot{\mathbf{D}}\}+[\mathbf{K}]\{\mathbf{D}\}=0 \quad \ldots (5)$$

Nodal displacements and accelerations associated with the free harmonic oscillation can be written as

$$\{\mathbf{D}\}=\{\bar{\mathbf{D}}\}\,\text{Sin}\omega t \quad \ldots (6)$$

$$\{\ddot{\mathbf{D}}\}=-\omega^2\{\bar{\mathbf{D}}\}\,\text{Sin}\omega t \quad \ldots (7)$$

where $\{\bar{D}\}$ represents the variation of nodal displacements from static equilibrium. Substitution of Equations (6) and (7) into Equation (5) yields the eigenproblem for undamped free vibration of a multiple degree of freedom system:

$$\left([\mathbf{K}]-\omega^2[\mathbf{M}]\{\bar{\mathbf{D}}\}\right)=\{0\} \quad \ldots (8)$$

where ω^2 is an eigenvalue and ω is one of the natural frequencies of vibration. It is of fundamental importance to know the normal modes of a structure since its deformation is a maximum for these mode shapes. It is also used to indicate the best location for the piezoelectric patches. ANSYS® modal analysis provides these natural frequencies of vibration as well as the corresponding mode shapes. Block Lanczos method was used for the solver since it performs well when the model consists of poorly shaped shell and solid elements as is the case of the present study.

4.1.2 Aerodynamic coupling

The aerodynamic coupling is performed using ZAERO® module for flutter analysis through ZONA6 Unsteady Subsonic Aerodynamics Code which is presented in the Zona ZAERO® Theoretical Manual[16]. In order to generate the flutter solution, a modal AIC (Aerodynamic Influence Coefficient) matrix relating structural mode shapes to unsteady aerodynamic forces must be calculated. By multiplying the area of each box of the plate by the unsteady pressure on that box, the normal force may be computed. After expanding the normal force vector to include the force and moment components, a square matrix relating the structural mode shapes to the aerodynamic forces is constructed as

$$\{\mathbf{L}_{\mathbf{h}}\}=q_\infty[\mathbf{AIC}]\{h\} \quad \ldots (9)$$

where $\{L_h\}$ is the resultant aerodynamic force vector at each aerodynamic box due to h, q_∞ is the freestream dynamic pressure and $\{h\}$ is the structural deformation of each aerodynamic box.

The general system of equations for flutter in the Laplace domain may be written as;

$$[s^2\,\mathbf{M}=s\mathbf{C}=\mathbf{K}]q=F_a \quad \ldots (10)$$

where $M=\Phi^T m\Phi$ is the generalised mass matrix, $K=\Phi^T k\Phi$ is the generalised stiffness matrix, $C=\Phi^T c\Phi$ is the generalised viscous damping matrix, q are the generalised co-ordinates, and F_a are the aerodynamic forces produced by structural deformation.

This equation is solved in ZAERO® using the *k*-method and the *g*-method. The *k*-method of flutter analysis considers the aerodynamic loads as complex masses, and the flutter analysis becomes a vibration analysis using complex arithmetic to determine the frequencies and artificial damping required to sustain the assumed harmonic motion. The *k*-method of flutter analysis is a looping procedure. The values of V, g, and f are solved for various values of m, k, and ρ. Plots of V versus g can be used to determine the flutter speed[17] (where damping goes through zero to positive values). In the *g*-method, the first order damping is derived from Laplace domain unsteady aerodynamic forces. The flutter boundary is provided when the value of damping is equal to zero. A technique of reduced frequency sweeps is then introduced. This technique seeks the condition where the damping is zero by solving the eigenvalues. The sweeping starts from zero reduced frequency of the unsteady aerodynamic forces with an increment value defined by the user and stops at its maximum value. The frequency and damping is then obtained. Then, the *V-f* and *V-g* curves can be plotted.

Both methods make use of the assumption that, at the flutter boundary, one of the natural vibration modes of the system will become neutrally stable and produce simple harmonic motion and the other modes remain stable.

4.2 Flutter results

As mentioned above, three plates with different materials were considered in this study, all having dimensions 500mm × 150mm and being built-in at one of the shorter sides. The sandwich plate has a 1mm thick cork core and one 0·2mm layer of woven carbon/epoxy at each of the facings. The other two are 6061-T6 aluminium alloy and carbon-epoxy plates with thickness of 0·75mm and 1·4mm, respectively. The material and geometric properties of each plate are summarised in Table 3.

The sandwich modelling capacity of ANSYS® was used with 2D SHELL91 elements. This element allows a layer by layer definition of the core and facings, defining individually the thickness and material properties of each of the sandwich constituents. It is also suitable for relatively thick cores relative to the facings of the sandwich. Cantilever boundary conditions were defined and the modal analysis was performed in order to retrieve the natural frequencies and mode shapes of the structure. The first ten mode shapes of the carbon-cork sandwich are illustrated in Fig. 9.

The structural modal data was exported to ZAERO® to perform the aerodynamic coupling, considering the conditions defined in the input file, namely aerodynamic mesh density, sea level conditions, etc.

https://doi.org/10.1017/S0001924000006205 Published online by Cambridge University Press

Table 3
Material and geometrical properties of plates considered in the flutter analysis

Material Properties

	Aluminium	Carbon/Epoxy	Cork
E_x, GPa	68·9	42	0·032
E_y, GPa	–	42	0·032
G_{xy}, GPa	–	5	0·005
υ	0·33	0·1	0·26
ρ, kg/m^3	2,800	1,400	300

Geometrical Properties

	Aluminium	Carbon/Epoxy	Sandwich
Span, m	0·5	0·5	0·5
Chord, m	0·15	0·15	0·15
Thickness, mm	0·75	1·40	1·40

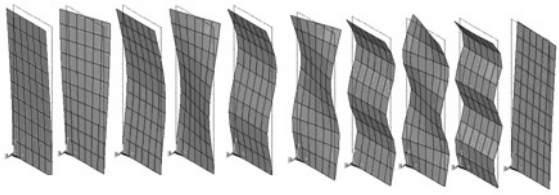


Figure 9. First ten modes of vibration of sandwich plate.

After running the aeroelastic code, the cork sandwich flutter mode representation was obtained at the flutter speed of 19·91ms^{-1}. This flutter mode has the contribution of the first bending mode (14·86%) and the first torsion mode (100%). This means that, if the structure did not have the first bending mode, its flutter behaviour would change slightly whilst in the absence of the torsion mode its behaviour would change dramatically.

Figure 10(a) represents the *V-g* diagram for the plates with different materials. Positive and negative damping values are representative of unstable and stable conditions, respectively. As we can see, flutter occurs when the velocity curve intercepts the zero damping line. This means that at this velocity, if the structure suffers an excitation, the aerodynamic flow will no longer damp the structural vibration. One is then able to determine the flutter frequency of the model using the plot of Fig. 10(b) and picking off the frequency value of the unstable mode at the flutter velocity value. The slope of the damping versus velocity curve as it passes through flutter velocity can be thought of as a qualitative measure of how violently the oscillations would occur during accelerated flight.

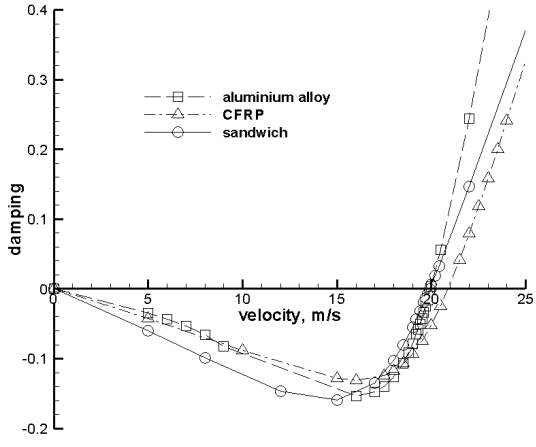
We can clearly see that although the three plates are limited by the same flight envelope, the cork sandwich ensures a lighter structure and, therefore, a higher flutter speed to mass ratio as it is shown in Table 4. This is due to the fact that the higher second moment of area provided by the sandwich and its comparatively low weight shifts the natural frequencies of the first bending and torsion modes, the most critical ones, to higher values as represented in Fig. 10(b) and quantified in Table 5.

It is interesting to notice, however, that even with the same thickness, without the second moment of area taking a predominant role, the sandwich structure ensures practically the same flight envelope than the carbon-epoxy plate, although with a much lower weight.

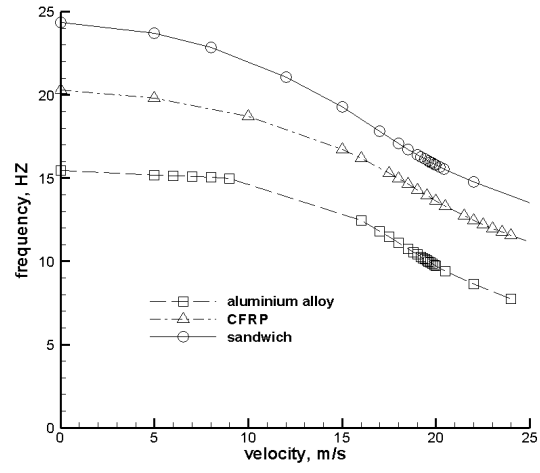
Table 4
Flutter analysis results for all three plates

	Aluminium (0·75mm)	**CFRP (1·4mm)**	**Sandwich (1·4mm)**
V_f *g*-method, ms^{-1}	19·98	20·87	19·92
V_f *k*-method, ms^{-1}	20·00	20·90	19·80
Flexural rigidity*, N.m^2	0·363	1·44	0·916
Specific rigidity, N.m^5/kg	1·30e^{-4}	1·03e^{-3}	1·49e^{-3}
Mass, kg	0·158	0·116	0·065
V_f/Mass, m.s^{-1}/kg	125·8	180·17	306·5

*The flexural rigidity is denoted by EI, where E is the Young's modulus and I is the second moment of area.



(c)



(d)

Figure 10. Damping and frequency results for all three plates: (a) *V-g* diagram and (b) *V-f* diagram.

https://doi.org/10.1017/S0001924000006205 Published online by Cambridge University Press

Table 5
First four natural frequencies of vibration in Hz

Mode	Aluminium	CFRP	Sandwich
1	2·46	4·61	5·97
2	15·48	18·86	24·36
3	16·54	28·86	37·38
4	43·81	61·99	80·03

5.0 CONCLUSIONS

In the first part of this work, the damage tolerant properties of cork based composites were assessed through low velocity impact testing. Experimental results allow concluding that:

- The use of cork-epoxy agglomerates as a core material in sandwich components is a viable alternative to other low weight materials (such as polymeric foams) with enhanced damage tolerant characteristics. In fact, results from the impact tests are conclusive about the superior energy absorption properties of cork based composites, which have an inferior extension of damage of both the core and facesheet materials when compared with PMI foams;
- Residual strength flexural tests after impact demonstrate that cork based sandwich components are less susceptible to the damage caused by impact events with different levels of energy, as they withstand higher values of ultimate load when compared with PMI specimens;
- The use of embedded cork granulates in carbon-epoxy laminates improves the resilient properties of this usually brittle type material. Impact tests show that cork based laminates have an higher level of absorbed energy, which means that they have a superior damage tolerance when compared with plain carbon-epoxy laminates;
- The observation of the cross-section of the impacted specimens confirm the lesser extension of internal damage in the cork based laminates, which can be attributed to an arresting effect of the cork layer to the progression of the impact waves.

In the second part of this work, the passive flutter behaviour of carbon-cork sandwich, conventional carbon-epoxy and aluminium plates were compared. It has been shown that the cork sandwich can provide the same flight envelope for a lighter structure. This is due to the fact that the second moment of area is increased by a thicker structure with reduced weight owing to the low density of cork. Although this outcome was expected for such a structure configuration, the use of cork-based sandwiches for improving vibration damping in aeronautical applications subject to flutter oscillation requires further investigation.

REFERENCES

1. BAKER, A., DUTTON, S. and KELLY, D. (Eds), *Composite Materials for Aircraft Structures*, AIAA, Reston, USA, 2004.
2. RICHARDSON, M.O.W. and WISHEART, M.J. Review of low-velocity impact properties of composite materials, *Composites Part A 1996*, **27A**, pp 1123-1131.
3. NIGAM, V., SETUA, D.K. and MATHUR, G.N. Failure analysis of rubber toughened epoxy resin, *J Applied Polymer Science*, 2003, **87**, pp 861–868.
4. RUKSAKULPIWAT, Y., SRIDEE, J., SUPPAKARN, N. and SUTAPUN, W. Improvement of impact property of natural fiber–polypropylene composite by using natural rubber and EPDM rubber, Composites: Part B, 2009, **40**, pp 619-622.
5. HEDRICK, J.C., NIRANJAN, M.P. and MCGRATH, J.E. Toughening of epoxy resin networks with functionalized engineering thermoplastics, *Advances in Chemistry*, 1993, **208**, pp 293-304.
6. GIL, L. Cork composites: a review, *Materials*, 2009, **2**, pp 776-789.
7. SILVA, S.P., SABINO, M.A., FERNANDES, E.M., CORRELO, V.M., BOESEL, L.F. and REIS, R.L. Cork: properties, capabilities and applications, *International Materials Reviews*, 2005, **50**, (6), pp 345-365.
8. PETIT S., BOUVET C., BERGEROT A. and BARRAU J-J. Impact and compression after impact experimental study of a composite laminate with a cork thermal shield, *Composites Science and Technology*, 2007, **67**, pp 3286-3299.
9. VINSON, J.R. *The Behaviour of Sandwich Structures of Isotropic and Composite Materials*, Technomic Publishing Co Inc., Lancaster, USA, 1999.
10. ZENKERT D. *The Handbook of Sandwich Construction*, North European Engineering and Science Conference Series, EMAS Publishing, Cradley Heath, 1997.
11. SILVA, J.M., DEVEZAS, T., SILVA, A., GIL, L., NUNES, C. and FRANCO, N., Exploring the use of cork based composites for aerospace applications, Materiais 2009, 5th International Materials Symposium – Recent Advances in Characterization, Processing, Design and Modelling of Structural and Functional Materials, SPM, IST – Lisbon, Portugal, 5-8 April 2009.
12. CASTRO, O, SILVA, J.M., DEVEZAS, T., SILVA, A. and GIL., L. Cork agglomerates as an ideal core material in lightweight structures, *Materials and Design*, 2010, **31**, pp 425-432.
13. ASTM C393/C393M–06, Standard Test Method for Core Shear Properties of Sandwich Constructions by Beam Flexure, *Book of Standards*, **15.03**, ASTM International, West Conshohocken, 2006.
14. ASTM D7136/D 7136M-07, Standard Test Method for Measuring the Damage Resistance of a Fiber-Reinforced Polymer Matrix Composite to a Drop-Weight Impact Event, Book of Standards, Volume 15.03, ASTM International, West Conshohocken, 2007.
15. ASTM International D790-03, Standard Test Methods for Flexural Properties of Unreinforced and Reinforced Plastics and Electrical Insulating Materials, Book of Standards, Volume 8.01, ASTM International, West Conshohocken, 2003.
16. Zona Technology Inc., ZAERO Applications Manual Version 4.1, Zona Technology Inc., Scottsdale, USA, 2000.
17. RODDEN, W.P. and JOHNSON, E.H., MSC NASTRAN Aeroelastic Analysis User's Guide v68, MSC Software Corporation, Santa Ana, USA, 2004.

https://doi.org/10.1017/S0001924000006205 Published online by Cambridge University Press